Chaos, Solitons and Fractals 210 (2026) 118671

Contents lists available at ScienceDirect

Chaos, Solitons and Fractals

journal homepage: www.elsevier.com/locate/chaos

The effect of HVDC lines in power-grids via Kuramoto modelling

Kristóf Benedek [a,b,*], Géza Ódor [a]

[a] Institute of Technical Physics and Materials Science, HUN-REN Centre for Energy Research, Konkoly-Thege Miklós út 29-33, P.O. Box 49, Budapest, H-1525, Hungary

[b] Department of Theoretical Physics, Institute of Physics, Budapest University of Technology and Economics, Műegyetem rkp. 3, Budapest, H-1111, Hungary

ARTICLE INFO

Keywords:
Synchronization
Second order Kuramoto model
Heterogeneity
Power-grids
HVDC

ABSTRACT

We present a numerical study on the synchronization and cascade failure behaviour by solving the adaptive second-order Kuramoto model on a large high voltage (HV) European power-grid. This non-perturbative analysis takes into account non-linear effects, which occur even when phase differences are large, when the system is away from the steady state, and even during a blackout cascade. Our dynamical simulations show that improvements in the phase synchronization stabilization as well as in the cascade sizes can be related to the finite size scaling behaviour of the second order Kuramoto on graphs with $d_s < 4$ spectral dimensions. On the other hand, drawbacks in the frequency spread and Braess effects also occur by varying the total transmitted power at large and small global couplings, presumably when the fluctuations are small, causing a freezing in the dynamics. We compare simulations of the fully AC model with those of static or adaptive High Voltage Direct Current (HVDC) line replacements. The adaptive (local frequency difference-based) HVDC lines are more efficient in the steady state, at the expense of very long relaxation times.

1. Introduction

Power-grids make up one of the most important infrastructures of technological civilization as they distribute the energy from resources to consumers. They are organized into the largest man-made synchronous machines as they are based on oscillatory elements, related to the traditional rotating generator sources and mechanical machines.

However, nowadays this is about to change with the extension of renewable resources and other consumers which cannot be considered simple oscillators (see [1]). To balance supply and demand, highly synchronized, continent-sized grids have been created, in which the phase differences drive the flow of energy from one node to the other. This permits describing classical power-grids by the so-called swing equations [2], equivalent to the second (or higher) order Kuramoto model (KM) equations [3], exhibiting inertia.

The second-order Kuramoto model provides a simplified yet qualitatively correct dynamical description of power-grid frequency dynamics under several assumptions: voltage magnitudes are considered constant, reactive power dynamics are neglected, and the dominant interactions arise from phase differences between connected nodes. Under these approximations, the swing equations reduce to coupled oscillator dynamics, where generators and loads are represented as phase oscillators with inertia.

While the Kuramoto framework captures important aspects of synchronization dynamics in power systems, it still is a simplified model of real grid operation. Several physical parameters of the European grid are not publicly available and therefore must be

* Corresponding author at: Institute of Technical Physics and Materials Science, HUN-REN Centre for Energy Research, Konkoly-Thege Miklós út 29-33, P.O. Box 49, Budapest, H-1525, Hungary.

E-mail addresses: benedek.kristof@ek.hun-ren.hu (K. Benedek), odor.geza@ek.hun-ren.hu (G. Ódor).

https://doi.org/10.1016/j.chaos.2026.118671
Received 12 January 2026; Received in revised form 16 March 2026; Accepted 13 June 2026

Available online 24 June 2026

approximated or modelled; consequently, an exact description is impossible due to a lack of knowledge and data as well. As a result, the present study should be interpreted primarily as a conceptual and qualitative investigation of topology-driven synchronization exploring how simple modelling of HVDC connections can alter the behaviour of the traditionally fully AC power-grid.

Inertia traditionally comes from rotating masses. By introducing elements based on new technology (e.g. renewable energy sources, direct current (DC) lines, etc.), this inertia is being reduced. Therefore, power grids become more vulnerable, since with the reduction of the rotating inertia, smoothening perturbations in the power flow and frequency is decreasing. Because of this, instabilities and abrupt changes are not damped spontaneously. The instabilities can arise from multiple sources, be it a change in demand and supply in different regions [4], operator mistakes, system failures, solar flares and many more. Due to the integration of renewables, the system is also subject to the big energy fluctuations due to weather, amplified by climate change [5]. Large fluctuations in the frequency lead to the disintegration of the synchronization, cascade failures and blackouts [6].

There are several attempts to mitigate these fluctuations: addition of inertia at critical places [7], usage of adaptive inertia [8], and another solution is the application of direct current (DC) lines partitioning the power-grid into smaller parts [9]. This technology is well-known and used in the case of high-power and long-distance (typically seabed) cables, as energy can be transmitted more efficiently over them than via alternating current (AC) ones.

Recent operational experience further underlines the stabilizing potential of HVDC-based separation. During the 28 April 2025 Iberian blackout, HVDC interconnections limited the propagation of frequency and angle disturbances between the Iberian Peninsula and the rest of continental Europe, effectively decoupling unstable dynamics while maintaining controlled power exchange [6]. This illustrates how HVDC links can act as dynamical firebreaks in large synchronous systems.

It is also known that altering of power-grid structure and/or parameters do not always lead to improved performance, even if they are planned to be like that. In particular, the Braess paradox [10,11] can occur by transmission line improvements, for example by adding new lines or additional capacity. Such effects have been discussed previously in the context of power-grid synchronization models [12–14]. In the present work, we therefore investigate whether introducing HVDC connections within the framework of the second-order KM with different power control across them can produce similar non-trivial trade-offs in synchronization properties and cascade robustness.

Synchronization transitions are related to the spectrum of the Laplacian matrix of complex networks. The normalized Laplacian matrix defined as $L_{ij} = \delta_{ij} - A_{ij}/k_i$, where δ_{ij} denotes the unit, A_{ij} the adjacency matrices and k_i is the degree of node i. As linearized KM equations describe random walks, the eigenvalue spectra of L_{ij} encodes the dimensionality information of a network related to synchronization as well [15]. In particular the density of the smallest eigenvalues can be characterized by the following scaling behaviour [15,16]

$$\rho(\lambda) \simeq \lambda^{d_s/2-1} \tag{1}$$

for $\lambda \ll 1$, providing a definition for the spectral dimension d_s.

We know that power-grid topologies are characterized by rather low spectral dimension (d_s) [17]. At $d_s < 4$ dimensions real synchronization phase transition of the KM order parameter cannot happen and even frequency entrainment phase transition does not occur for $d_s < 2$. That does not exclude partial synchronization with a crossover phenomenon; however, that means that the coupling strength K_c where synchronization reaches a certain degree grows and diverges with the system size by the laws shown by Ref. [18] on regular lattices. As a consequence, smaller systems exhibit smaller K_c, but higher order parameter values, thus the DC separation of a power-grid graph must lead to sub-systems with higher synchronization order parameter values for a given K.

In this study, we show on a real[1] European high voltage HV power-grid (from 2016) the solution of the adaptive KM, which involves co-evolution of the network with an overload condition, how the application of different HVDC methods modify the synchronization and cascade failure behaviour. Static and adaptive HVDC methods are compared, which introduce further network changes dynamically. Our work and results complement existing electrical engineering (EE) work from a deeper, physics-based perspective.

2. Previous works

There seems to be at least two sides of the HVDC separation advantages:

- reduction of cascade failures, which can be taken into account even by DC load models.
- improvement of synchronization measures (and stability), which can be modelled by AC–DC models.

At first glance, one may assume that large power systems allow the possibility to balance between energy demand and resources, thus they provide more stability for power-grids. However, recent studies have demonstrated that this is not always the case, and segmentation of power systems can be advantageous [20,21]. An early study, based on a risk assessment method, has shown that HVDC segmentation can significantly reduce the risk of cascading failures [22]. This model is based on the simple fact that cascading outages and collapse will be limited to only one segment, which reduces the risk of widespread blackout. Several variants of simple DC/EE models have been designed and investigated to prove this.

[1] By real we mean, that the topology of the network corresponds to reality, the weights of the lines were set with respect to the actual capacity, voltage level and reactance of the lines as per described in [19].

In the study of synchronization and stability in large power networks, prior work mainly relies on two modelling paradigms: *load-flow/OPF-based methods* and *OPA-type cascading-failure models*. Optimal power-flow (OPF) formulations based on AC or DC load flow remain the standard for characterizing feasible steady-state operating points under network constraints [23,24]. They also provide the operating equilibria from which linearized small-signal stability or nonlinear swing-equation studies are conducted. Such OPF-derived operating points have been extensively used in research on grid synchronization, stability margins, and vulnerability to large transfers in meshed transmission systems [25–27].

Complementing these approaches, the *ORNL–PSERC–Alaska (OPA)* model [28,29] offers a coarse-grained representation of cascading failures based on a DC load-flow approximation. Its stochastic outage rules and slow-timescale adaptation enable the study of large blackout statistics and systemic risk. The recent application of OPA to the European transmission grid [9] demonstrates how splitting the system into asynchronously coupled regions via HVDC corridors can reduce large-scale cascading risk in an economically favourable manner. However, because OPA relies on a *fully DC approximation*, it cannot capture angle-dynamics, reactive-power effects, or loss-of-synchrony phenomena in the AC system.

Across both OPF-based and cascading-risk models, *HVDC interconnections* are typically represented as controllable power-transfer elements that fully decouple AC phase angles. In steady-state load-flow and OPF formulations, an HVDC link is usually modelled as two converter terminals enforcing specified injections, accompanied by converter losses and operational limits [30]. In stability-focused studies and synchronization modelling, HVDC links appear as idealized controllable injections that do not transmit inertia or synchronizing torque, thereby enabling regional decomposition of the AC grid. This abstraction captures the essential feature that HVDC allows power sharing without enforcing frequency or phase synchrony, making it a suitable tool for mitigating cascading failures or intentionally segmenting large synchronous areas [31,32].

Another recent work has analysed the synchronous AC grid of continental Europe under tunable large inter-regional power flows [4]. This study starts from the AC swing equations and applies a linear stability approximation to identify critical lines in the EU and develops a numerical approach to force the splitting of the AC grid into disconnected areas. This is basically also a load-flow-driven model in which "HVDC-like" decoupling is emulated by cutting lines whose phase difference saturates, i.e. $|\theta_i - \theta_j| > \pi/2$.

Complementary to segmentation, modern control seeks to compensate lost inertia and stabilize frequency. Adaptive (time-varying) synthetic inertia was shown to suppress coherency oscillations and improve stability margins in high-renewables grids [33]. There is also progress on where to place inertia: optimization on second-order Kuramoto dynamics with threshold-based tripping suggests that *where* inertia is added matters as much as *how much*, with peripheral placements often outperforming central ones [7].

We will investigate this problem via the extension of the second order Kuramoto (AC–DC) model with an underlying line-failure dynamics, which can treat both sides, without using a linear approximation. This can be interesting in light of the 2025 Iberian blackout, which has renewed attention to voltage/frequency stability and the role of inter-area separation and controls at scale [6].

3. Models and methods

3.1. Dynamical simulations of the AC power-grid via Kuramoto model

The dynamics of the power-grid built up for mechanical elements (e.g. rotors in generators and motors) can described by the swing equations [2]. It is equivalent to the Kuramoto equation of second type [3] possessing inertia, which can be set up for a network, containing N oscillators with phase variables $\theta_i(t)$. We use here a specific form, including dimensionless electrical parameters and approximations for the unknown quantities as in [19,34–36],

$$\ddot{\theta}_i + \alpha\ \dot{\theta}_i = P_i + \frac{P_i^{max}}{I_i\ \omega_G}\ \sum_{j=1}^{N} W_{ij}\ \sin\left(\theta_j - \theta_i\right)\ . \tag{2}$$

Here α denotes the damping factor, which describes the power dissipation, or instantaneous feedback [37], $K := P_i^{max}$ is a global control parameter, related to the maximum transmitted power between nodes, $I_i = I$ is the inertia and ω_G describes the generator frequency, which are assumed to be constants in the lack of our knowledge. W_{ij} denotes the weighted adjacency matrix of the network, containing admittances, calculated from line susceptances as described in [19]. The fixed external drive, denoted by $P_i := \omega_i^0$, corresponds to the self-frequency of the ith Kuramoto oscillator, describes the input–output powers of the nodes.

Here, in the absence of our knowledge of the input–output nodal powers, self-frequencies, are set to be random variables, drawn from a zero-centred Gaussian ensemble.[2] Note, that the rescaling invariance of Eq. (2) allows to transform these in a rotating frame to obtain other, variable nodal power values (see [36]). We also assumed that the initial frequencies of the nodes $\omega_i(0)$ are the same as their self-frequencies: $\omega_i(0) = \omega_i^0$. In this study the following damping parameter setting was used for the dissipation factor $\alpha = 0.4$, which is common in real power-grid models, when they are parametrized with real physical dimensions [12], but this can also be transformed via the rescaling invariance of Eq. (2) to other values.

To integrate the differential equations we used the adaptive Bulirsch–Stoer stepper [38] in the case of the GPU code, while running on CPUs we used the adaptive step-sized fourth-order Runge–Kutta method [39]. The nonlinearity in Eq. (2) introduces chaos, which can be regarded as a 'noise', even without stochasticity, and due to this a desynchronization transition occurs by lowering K from high values. The solutions depend on the actual quenched ω_i^0 self-frequency realization and to achieve reasonably

[2] Zero-centredness assures energy conservation across the grid.

small fluctuations of the averages of the measured quantities, we needed strong computing resources, generally parallel codes running on GPU HPC machines. As Eq. (2) exhibits a first order transition with metastable solutions even in the long-time limit, to obtain stronger synchronization solutions, the initial state was set to be phase synchronized: $\theta_i(0) \simeq 0$.

We measured the standard, complex valued KM phase order parameter

$$z(t_k) = 1/N \sum_j \exp\left[i\theta_j(t_k)\right] \ . \tag{3}$$

Since $z(t_k)$ is a complex-valued number, the phase alignment at a given time t_k is given by its modulus:

$$r(t_k) = |z(t_k)| \ . \tag{4}$$

We also computed a topology respecting order parameter introduced by Schröder et al. [40]:

$$r_{uni}(t_k) = 1/(\sum_{i,j}^{N} W_{ij}) \sum_{i,j}^{N} W_{ij} \cos(\theta_i - \theta_j) \ , \tag{5}$$

which describes the energy of classical rotator models (eg. XY model) and the variance of the frequencies :

$$\omega(t_k) = \frac{1}{N} \sum_{j=1}^{N} (\overline{\omega}(t_k) - \omega_j(t_k))^2 \ , \tag{6}$$

where $\overline{\omega}(t_k)$ denotes the spatial average at time t_k. Sample averages for the Kuramoto order parameter:

$$R(t_k) = \langle r(t_k) \rangle \ , \tag{7}$$

and for the topology respecting one we have:

$$R_{uni}(t) = \langle r_{uni}(t_k) \rangle \ , \tag{8}$$

and for the frequency variances

$$\Omega(t_k) = \langle \omega(t_k) \rangle \ , \tag{9}$$

were performed over hundreds of independent self-frequency realizations. As the self-frequencies generate a quenched disorder variances of the order parameters were also calculated without having stochastic noise. To save data storage and computing time the solutions were sampled at discrete, incremental time steps: $t_k = 1{+}1.08^k$, $k = 1, 2, 3$....in accordance with the relaxation behaviour worst near the synchronization transition point K_c.

We have extended the numerical solution equation of motions with a threshold dynamics, to model overflow of power on the edges that were removed during the simulation, generating a cascade failure. This method is similar to what was published in [36,41]. Following a thermalization to steady states, characterized by R, R_{uni}, Ω, initialized from phase-ordered states, which we inspected by plotting the order actual parameters, the systems were perturbed by removing a randomly selected edge, in order to simulate a power line failure event. Following that, if the ensuing power flow on a line between neighbouring nodes was greater than a threshold:

$$F_{ij} = |\sin(\theta_j - \theta_i)| > T \ , \tag{10}$$

the line was regarded as overloaded and we removed this link from the adjacency graph permanently (in run). In connection with this we calculated the total number of line failures $\langle N_f \rangle$ of the simulated blackout cascades of each realization, corresponding to different $\omega_i(0)$. Following the cascade simulations we applied histogramming to determine the probability distribution functions (PDFs) of N_f-s.

We have investigated various modifications of European power-grids introduced in a previous work [19]. These graphs are based on data from 2016 for Europe (EU2016) GridKitproject, which relies on the ENTSO-E's statistics for power generation and consumption, voltage levels; and data obtained from OpenStreetMap (.osm) files. These contain information on the topology, geographical coordinates of nodes, and lengths, types, voltage levels of cables. The EU2016 network contains $N = 13\,478$ nodes and $E = 18\,393$ bi-directional edges and a hierarchical modular structure [36]. Since we use publicly available .osm files, this implies, the data may be badly labelled, meaning there is a possibility of having missing data for certain grid elements, resulting in an incomplete dataset in terms of parameters. To resolve the problem, we made assumptions in [19] to substitute the missing data in order to obtain a fully weighted network. Furthermore, in [19] all connections were assumed to be AC like, even the DC line ones. The spectral dimension of the weighted graph was found to be $d \simeq 2.34$ [17]. In [19] a complete graph invariant and community structure analysis was also presented.

3.2. Including HVDC lines

In modern power systems, the use of HVDC transmission has emerged as a key solution for efficiently linking remote generation sites, interconnecting asynchronous grids and delivering bulk power via submarine or underground cables. Unlike the more conventional AC systems, an HVDC link carries electricity as direct current typically in the range of $100\,\mathrm{kV} - 800\,\mathrm{kV}$ which offers a

number of compelling advantages, such as lower transmission losses over long distances and the requirement of fewer conductors, since there are no three phases and no skin effect to worry about.

At the same time, HVDC cable systems are not without drawbacks. The terminal converter stations (AC↔DC and vice versa) are complex and expensive. For short transmission distances, the losses and cost of the conversion equipment may outweigh the savings in cable or line cost, meaning there is a so-called "break-even" distance beyond which HVDC becomes economical. Moreover, expanding DC systems into multi-terminal or meshed arrangements is still more challenging than with AC, because DC protection, switching, and converter coordination are more complex.

HVDC lines transmit power only; there is no phase or frequency information carried over. In the synchronization sense, they segment the network into distinct clusters. The key question arising when it comes to their modelling is how to implement regularization of the power. This can be done in several ways [42,43]:

1. Converter control strategies
   (a) Voltage droop control: a proportional relationship between DC voltage and the required power.
   (b) Constant power control: when constant power is needed, independent of the voltage.
   (c) Deadband droop control: a mixture of the above two.
2. Grid control strategies
   (a) Centralized voltage control: It is based on how the voltage source converter (VSC) HVDC point-to-point connection[3] is operated [44].
   (b) Distributed voltage control: Instead of having only one converter that controls the DC voltage in the grid as in centralized voltage control, distributed voltage control applies voltage droop control to several converters.

Very often, droop control or constant power control is implemented. Droop control introduces adaptivity into the system. Since all these techniques depend on converters, which can be programmed, power control could be influenced by voltage angle phase differences or frequency differences. We implemented several methods for this adaptivity, based on the frequency. We were inspired by the fact, that synchronous control in power grids is realized via frequency tuning [45].

We included the adaptive control in the Kuramoto model by modifying Eq. (2) as follows:

$$\ddot{\theta}_i + \alpha\dot{\theta}_i = P_i + \frac{P_i^{max}}{I_i\,\omega_G} \sum_{j,\ \text{if edge is AC}} W_{ij} \sin\left(\theta_j - \theta_i\right) + \sum_{j,\ \text{if edge is DC}} f(\dot{\theta}_j - \dot{\theta}_i)\cdot D_{ij}\ . \tag{11}$$

Here we introduced a new term, in which D_{ij} is the strength of the HVDC link, proportional to the maximal transmissible power through it and $f(x)$ is a so-called *activation function* (c.f. Fig. 1), normalizing the frequency difference between -1 and 1. This adds a possibility to adaptively set the power flow across DC lines and can be further combined with static power control. It is important to stress that HVDC lines themselves do not transmit AC phase or frequency signals. Instead, the converters at the terminal buses implement a control strategy in which the transmitted power is adjusted based on the local frequency difference between the endpoints. We expect that via this term the grid gains a better ability to self-organize towards synchrony, visible in achieving higher R order parameter values, preferably lower Ω frequency spread and cascade sizes $\langle N_f \rangle$.

On the other hand, constant power control was also implemented and tested. To model this approach to HVDC lines, we removed these links from the graph by simply setting their weight $D_{ij} = 0$, realizing the grid segmentation as discussed before, and then we assumed that at the endpoints of these edges the nodes receive a specific input/output ($Pd_i = -Pd_o$) power(static HVDC).

In order to investigate the HVDC links across Europe, the first task was to identify the specific lines that were present in the ENTSO-E 2016 database, with their transmitted power. We decided to see the effects of replacing the seabed lines below the Baltic Sea. This amounts to 36 HVDC cables of the network, which is just 0.2% of the total, still has a large effect of decoupling the Scandinavian peninsula from the rest of the continent as shown on Fig. 2. Note, that some irrelevant DC substation nodes are not shown on the map and also dropped from the calculations.

It is crucial to acknowledge that in the absence of real power values of the EU2016 grid the Pd_i had to be properly normed to be in accordance with the randomly chosen generator and consumer values $P_i = \omega_o^0$, a zero-centred, random Gaussian values with unit variance ($\sigma = 1$). For the normalizing purpose of the HVDC node values, we used the nodal power values from [19] and assumed a correspondence between the 800 MV power with the $P_i = 3\sigma$. The real HVDC cables' power values were obtained from the ENTSO-E database and the $Pd_i = -Pd_o$ were calculated and used in the Kuramoto equations according to the above correspondence.

4. Results

This section presents our results for the EU2016 grid, where we implemented and tested various approaches to simulate HVDC connections. Earlier, we used an edge weighting method described in [19]. This involves grouping the edges according to voltage levels and assigning weights to the AC cables based on their voltages and susceptances. For DC cables, we assigned weights proportional to the total capacity.

[3] Typically used to connect the DC grid to weak and passive systems making it the best choice when connecting to e.g. offshore wind plants.

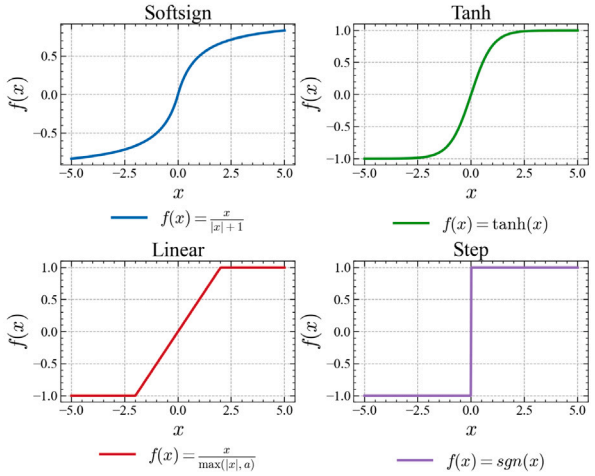

Fig. 1. Different types of activation functions used in the adaptive HVDC modelling scenarios.

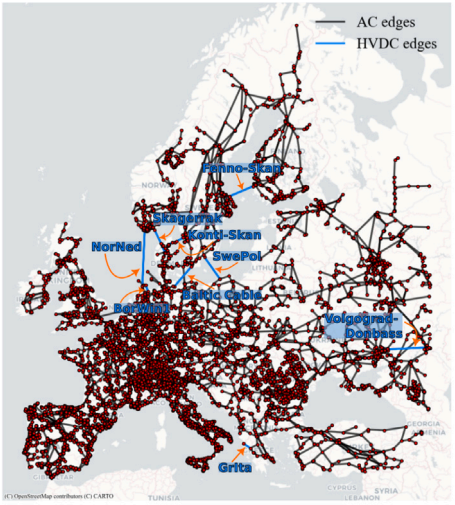

Fig. 2. HVDC cables in the continental European grid based on the 2016 data in GridKit. While the Baltic area is quite well documented, the Southern-Europe part is less so. In this work only the Baltic seabed cables were turned from AC to DC. (c.f. HVDC World map).

Investigating the EU2016 grid, we wanted to explore the impact of different activation functions (c.f. Fig. 1) and their parametrizations on the synchronization. In the domain of ENTSO-E, the power flow is regulated by Frequency Containment Reserves (FCR). FCR reacts to short-term frequency imbalances in the grid, the complete activation of the frequency reserve must be available within 30 s and cover a period of 15 min per incident according to ENTSO-E standards. Since HVDC elements can be viewed as building blocks segmenting the grid, they should be of key importance to balance out the power. However, the way they react to the frequency imbalances is encoded in the activation functions. In the electrical engineering context, FCR is realized via a linear function (Fig. 1, bottom left panel), that activates in a certain frequency band. The drawback is that this band has to be predefined and is arbitrary when it comes to theoretical investigation and modelling. Using $\tanh(x)$, $softsign(x)$ or $sign(x)$ functions has the natural benefit of not needing any additional parametrization. It has to be mentioned, that the $sign(x)$ function can cause very large transients towards the steady state, (see Fig. 3) since at balance, the frequency difference sign can tip from negative to positive at every iteration and vice versa, which can also lead to slow convergence of the adaptive solver. Since in the literature [43,45,46] HVDC elements are viewed as fine-tuning tools towards achieving better power flow and synchronization in the system, we test this theory via dynamical Kuramoto simulations. In Fig. 4, we show our results in the steady state after integrating Eq. (11) for 10 000 iteration steps in cases of full AC, HVDC static, linear, $\tanh(x)$ and $softsign(x)$ activations, and for $t_{max} = 300.000$ for the $sign(x)$ case. In the latter case, a much larger time was needed because of the aforementioned long transients. Nonetheless, each of the methods helps the synchronization to improve across the grid. In the case of the full AC model, the half $R(t)$ synchronization value is achieved at around coupling $K = 7000$. Simulations for the linear, $softsign(x)$ and the $\tanh(x)$ HVDC activations result in a

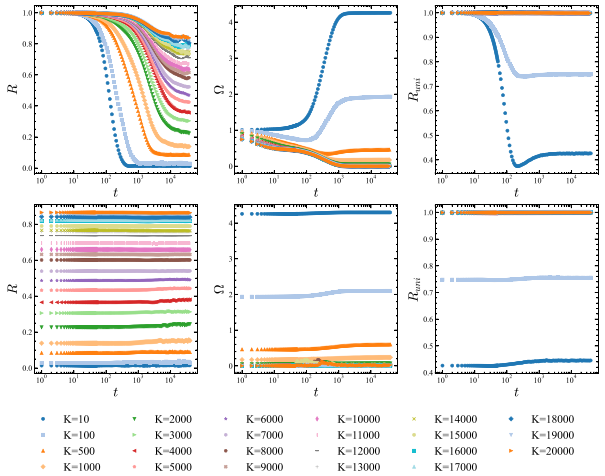

Fig. 3. Example timeseries for HVDC modelling with $softsign(x)$ function as activation. The top row displays the thermalization phase, and the bottom one corresponds to the cascade part of the simulations. We are showing results for our main synchronization metrics, $R(t_k)$, $\Omega(t_k)$ and $R_{uni}(t_k)$, for various global coupling values, marked by different colours and symbols. Saturation to the steady state values requires long times, typically 10^4 iterations and happens non-monotonically as we start from fully phase ordered initial states. The $R_{uni}(t_k)$ curves overlap above coupling $K = 500$, being a hallmark of good local synchronization. (For interpretation of the references to colour in this figure legend, the reader is referred to the web version of this article.)

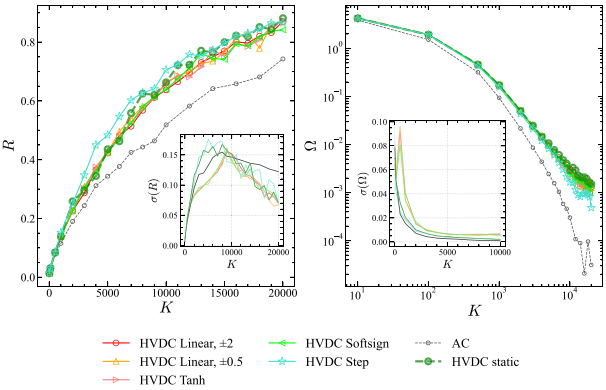

Fig. 4. Comparison of the steady state results after the thermalization of the fully AC and different HVDC approaches as the function of global coupling K in case of the EU2016 network. The inset shows the standard deviation of these quantities. Notice the fact that even static power input/output at DC buses helps the synchronization to improve. On the other hand, the frequency spread is increasing, which can be understood, since DC connections do not transfer phase information.

peaks in the $\sigma(R)$ at $K_c = 9000$, hallmark of the phase synchronization transitions at larger global power flows. On the other hand, the $sign(x)$ and the static DC functions decrease the peak locations to $K_c \simeq 5000$. Sample averaging was done over 200 random, independent self-frequency realizations.

On the second subplot of Fig. 4, we show the frequency spread results. As expected, in all of the HVDC modelling cases, this displays a higher value as compared to the full AC model. This can be understood, since DC connections do not transfer any phase and frequency related information between the two parts of the grid, only power. The total frequency distribution of the separated sub-networks can exhibit multi-peaks [47]. It was also shown in [18] that the frequency entrainment point $K_c'(N)$ also grows with the system size, and since $\Omega(N, K)$ is a monotonous function, for the sub-networks the $\Omega(N_{sub}, K) > \Omega(N, K)$ relation holds. Note, that we do not see peaks of the $\sigma(\Omega)$ curves because frequencies exhibit first order synchronization transition. We did not see much effect of HVDC lines with respect to the full AC on the R_{uni} steady state results, thus we omitted to plot this.

In the second part of our simulations, we created cascade events in the grid by manually cutting one of the randomly selected link in the steady state. This can lead to a domino effect of overloading lines by the condition Eq. (10), with $T = 0.99$ Note, these power-grid models exhibit rather strong inherent instabilities in the steady states for moderate couplings, thus we applied this high threshold value. Again, in the literature, it is claimed that HVDC links reduce the cascade risk, since they can respond rapidly to frequency oscillations and prevent failure propagation.

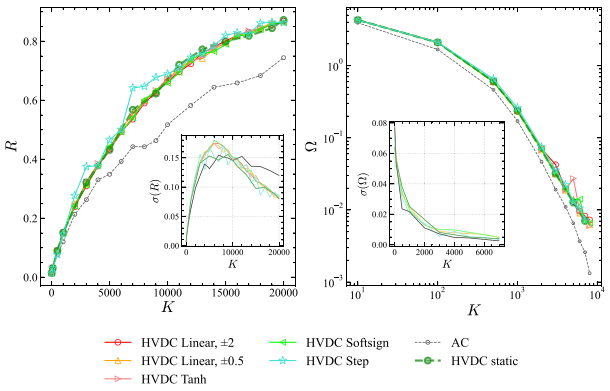

Fig. 5. Comparison of the dynamical cascade simulation results of the fully AC and different HVDC approaches as the function of global coupling K in case of the EU2016 network. The inset shows the standard deviation of these quantities. Even during cascade simulation, a higher synchronization is achieved when we account for the HVDC connections; however, the different approaches separate less than in the steady state (cf. Fig. 4). In terms of frequency spread the full AC model yields better results. This can be understood by the aforementioned fact that DC connections do not carry phase or frequency information, thus we divide the graph to smaller parts, in which these order parameters are higher.

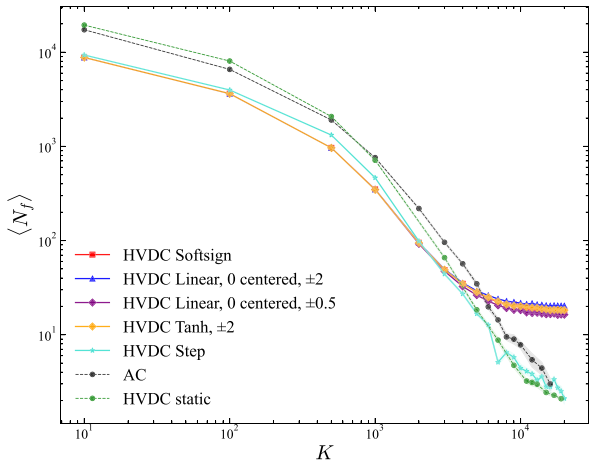

Fig. 6. Cascade size distributions for EU2016 with different types and valued activation functions in the HVDC cable terms compared to previous results, full AC simulation and static HVDC modelling. The shaded region represents the standard error corresponding to each case. Choosing the static modelling or $sign(x)$ as activation function, results in a stabilizing, cascade-reducing effect for all investigated K values. Other methods display a crossover behaviour, namely, they reduce the size distributions for lower couplings, but cannot mitigate the failures for higher values.

Like in case of the thermalization the dynamical cascade simulations were run until a steady state has been reached, determined by the order parameter differences, as shown on Figs. 3 and 5. While the static HVDC lines did not influence the relaxation times significantly, the adaptive ones can increase them drastically, making them 3 orders of magnitude larger. This is a natural consequence of the modelling. Taking for example, the linear activation function, as we decrease the interval for the linear part, we are turning the continuous equations into discontinuous ones, something that hinders all integrators in numerical methods.

We investigated the average size distribution of the cascade $\langle N_f \rangle$, as the function of the global coupling, for the different modelling scenarios, displayed on Fig. 6. We can see that linear activation, $\tanh x$ and $softsign(x)$ stabilizes the grid for K values up to 6000, but after that, they run into a saturation and cannot mitigate the cascade anymore.

In the case of the linear activation function (c.f. Fig. 1 bottom left panel), there is a possibility to vary the interval of the linear activation part. We kept the functions 0 centred, since the mean frequency, 50 Hz, can be transformed out from the Kuramoto equations Eqs. (2) and (11), but we experimented with various interval sizes. We display results only for some of the interval sizes in Fig. 6, ± 2, ± 0.5, but the dynamics were checked for other values, e.g. ± 1, ± 0.25, ± 0.1, too. The general conclusion of these results is that by decreasing the size of the interval (approaching the edge-case step function), we can push the saturation plateaus of $R(t)$-s and $N_f(t)$ lower, decreasing the cascade sizes in the system.

In the case of $sign(x)$ and static DC models, we see a stabilizing effect throughout the whole investigated coupling regime.

5. Conclusions

In conclusion, we presented dynamical cascade failure simulations on the EU2016 HV power-grid via the second order Kuramoto model by considering the effects of different HVDC separator lines between the Scandinavian Peninsula and the rest of the continent. The second order Kuramoto model is an appropriate representation of power grids of phase variables. In neglects the voltage amplitude variations (reactive power), phase delays and higher order interactions, which could be added via more complex, higher order approximations. Furthermore, we assumed that nodal power follows a random Gaussian distribution and a single-threshold failure mechanism. Our simplifications are standard in recent power-grid modelling [41] and we hope that extensions could be made on the expenses of more numerical efforts. The main point here was to link the existing results on the synchronization transitions on homogeneous lattices [18], with those obtained by more realistic simulations on the European HV power-grid topology. Furthermore, we could compare the effects of adaptivity with respect to static HVDC approach. Our method enables us to follow the evolution of synchronization behaviour deep in the non-linear regime permitting the determination of the steady state following a blackout cascade. Note, however that the conclusions may apply more to the topology-driven mechanisms of synchronous behaviour, rather than to actual cascade failure processes that involve complex protection systems and voltage stability.

The order parameter and the cascade size results could be interpreted by the knowledge of the second order Kuramoto model on graphs with spectral dimension $2 < d_s < 4$, where the synchronization crossover point moves to higher couplings as the function of size. As we replaced certain (0.02%) of the AC connections, by DC ones using sources and sinks at their end nodes we separated the graph into two smaller sub-graphs, thus both the Kuramoto and the frequency spread, defined by Eq. (9), order parameters move to higher values for a given K. This provides better phase, but worse frequency synchronizations at a given global power-level. Furthermore, the cascade sizes decrease for intermediate K-s, where the synchronization transition generates stronger fluctuations. Similar advances were found in case of line additions to the EU2016 grid, close to the synchronization transition coupling [13], where we argued about the positive effects of possible self-organized criticality. In the future, the effects of different additive stochastic noises should be investigated.

A comparison of static and different adaptive HVDC methods shows that the most sensitive, step-function, method provides the best results in the steady state. As our null model is the fully AC connected EU2016 power-grid from [13], the different HVDC modifications can also be considered as network developments, thus our results show ways to avoid the Braess paradox. According to our modelling HVDC lines generally improve phase synchronization, but also increase the frequency dispersion. Moreover, while adaptive HVDC may perform better in certain aspects, it leads to a significant increase in the relaxation time up to three orders of magnitude.

The significantly increased relaxation times observed for some adaptive HVDC schemes may also have practical implications. In real power systems, system operators rely on relatively fast stabilization of frequency and power flows after disturbances in order to avoid triggering additional protection mechanisms or control interventions. If the system relaxes too slowly, secondary disturbances or control actions may occur before the system has reached a new steady state, potentially complicating emergency response procedures.

Thus our results uncover an important trade-off to be made. While frequency stability (global synchrony) is vital for long-term balancing, phase synchronization (local synchrony) is critical within milliseconds to prevent immediate, severe disturbances. Phase synchronization should be prioritized over frequency dispersion (or maintaining exact frequency, as is done in long-term balancing) under circumstances where immediate, catastrophic physical damage to grid infrastructure is imminent, or when integrating low-inertia, high-variability renewable sources that threaten to tear the system apart.

Possible extension of this work would be the analysis of frequency distributions and comparison with real data.

CRediT authorship contribution statement

Kristóf Benedek: Writing – original draft, Visualization, Resources, Data curation. **Géza Ódor:** Writing – review & editing, Writing – original draft, Validation, Supervision, Project administration, Investigation, Funding acquisition, Conceptualization.

Software and third party data repository citations

The network data used for this study was based on the following sources: SciGRID project, Prebuilt Electricity Network for PyPSA-Eur based on OpenStreetMap Data [48], both being part of PyPsa-EUR [49]. For part of the simulations on GPU we used the KuramotoGPU code developed by Jeffrey Kelling, and for on CPUs we have used the code written by Kristóf Benedek and available via GitHub [50].

Declaration of competing interest

The authors declare the following financial interests/personal relationships which may be considered as potential competing interests: Kristof Benedek, Geza Odor reports financial support was provided by National Research Development and Innovation Office. If there are other authors, they declare that they have no known competing financial interests or personal relationships that could have appeared to influence the work reported in this paper.

Acknowledgements

We thank Jeffrey Kelling for creating and maintaining the KuramotoGPU HPC GPU code, Áron Weidinger and M. T. Cirunay for locating and calculating the EU2016 HVDC power lines, Pere Colet, Damia Gomilla and Bálint Hartmann for the useful comments and discussions. Kristóf Benedek acknowledges the support by the Doctoral Excellence Fellowship Programme (DCEP), founded by the National Research Development and Innovation Fund of the Ministry of Culture and Innovation and the Budapest University of Technology and Economics. Support from the Hungarian National Research, Development and Innovation Office NKFIH, Hungary (K146736) is also acknowledged.

Data availability

Data will be made available on request.

References

[1] ENTSO. Planning the future grid. 2024, https://tyndp.entsoe.eu/. [Accessed 17 February 2025].
[2] Grainger JJ, Stevenson WD. Power system analysis. McGraw-Hill; 1994.
[3] Filatrella Giovanni, Nielsen Arne Hejde, Pedersen Niels Falsig. Analysis of a power grid using a Kuramoto-like model. Eur Phys J B 2008;61(4):485–91.
[4] Martínez-Barbeito María, Gomila Damià, Colet Pere, Fritzsch Julian, Jacquod Philippe. Transmission grid stability with large interregional power flows. Phys Rev Res 2025;7:013137.
[5] Stürmer Julian, Plietzsch Anton, Vogt Thomas, Hellmann Frank, Kurths Jürgen, Otto Christian, Frieler Katja, Anvari Mehrnaz. Increasing the resilience of the texas power grid against extreme storms by hardening critical lines. Nat Energy 2024;9(5):526–35.
[6] ICS Investigation Expert Panel, European Network of Transmission System Operators for Electricity (ENTSO-E). Grid incident in Spain and Portugal on 28 April 2025: Factual report. Technical report factual report, Brussels, Belgium: ENTSO-E; 2025, Accessed: 2025-01-09.
[7] Park Sangjoon, Kim Cook Hyun, Kahng B. Optimal location of reinforced inertia to stabilize power grids. Chaos Solitons Fractals 2025;199:116768.
[8] Fritzsch Julian, Jacquod Philippe. Stabilizing large-scale electric power grids with adaptive inertia. PRX Energy 2024;3:033003.
[9] Gomila Damià, Carreras Benjamín A, Reynolds-Barredo José-Miguel, Martínez-Barbeito María, Colet Pere, Gomis-Bellmunt Oriol. Reducing blackout risk by segmenting European power grid with HVDC lines. J Mod Power Syst Clean Energy 2025;13(5):1556–67.
[10] Braess Dietrich. Über ein Paradoxon aus der Verkehrsplanung. Unternehmensforschung 1968;12(1):258–68.
[11] Braess Dietrich, Nagurney Anna, Wakolbinger Tina. On a paradox of traffic planning. Transp Sci 2005;39(4):446–50.
[12] Hartmann Bálint, Ódor Géza, Benedek Kristóf, Papp István, Cirunay Michelle T. Quantitative comparison of power grid reinforcements. Chaos Solitons Fractals 2025;200:117095.
[13] Ódor Géza, Papp István, Benedek Kristóf, Hartmann Bálint. Improving power-grid systems via topological changes or how self-organized criticality can help power grids. Phys Rev Res 2024;6(1):013194.
[14] Schäfer Benjamin, Pesch Thiemo, Manik Debsankha, Gollenstede Julian, Lin Guosong, Beck Hans-Peter, Witthaut Dirk, Timme Marc. Understanding Braess' paradox in power grids. Nat Commun 2022;13(1):5396.
[15] Burioni Raffaella, Cassi Davide. Universal properties of spectral dimension. Phys Rev Lett 1996;76(7):1091.
[16] Millán Ana P, Torres Joaquín J, Bianconi Ginestra. Complex network geometry and frustrated synchronization. Sci Rep 2018;8(1):1–10.
[17] Deng Shengfeng, Ódor Géza. Chimera-like states in neural networks and power systems. Chaos 2024;34(3):033135.
[18] Ódor Géza, Deng Shengfeng. Synchronization transition of the second-order Kuramoto model on lattices. Entropy 2023;25(1):164.
[19] Hartmann Bálint, Ódor Géza, Papp István, Benedek Kristóf, Deng Shengfeng, Kelling Jeffrey. Dynamical heterogeneity and universality of power-grids. Sustain Energy Grids Netw 2024;39:101491.
[20] Carreras BA, Newman DE, Dobson Ian. Does size matter? Chaos 2014;24(2):023104.
[21] Fairley Peter. Why Southern China broke up its power grid [news]. IEEE Spectr 2016;53(12):13–4.
[22] Mousavi OA, Bizumic L, Cherkaoui R. Assessment of HVDC grid segmentation for reducing the risk of cascading outages and black-outs. In: 2013 IREP symposium - bulk power system dynamics and control - IX optimization, security and control of the emerging power grid. Rethymno; 2013, p. 1–6.
[23] Kundur Prabha. Power system stability and control. McGraw-Hill; 1994.
[24] Sauer Peter W, Pai MA. Power system dynamics and stability. Prentice Hall; 1998.
[25] Dörfler Florian, Bullo Francesco. Synchronization in complex oscillator networks and smart grids. Proc Natl Acad Sci 2013;110(6):2005–10.
[26] Motter Adilson E, Myers Seth A, Anghel Marian, Nishikawa Takashi. Spontaneous synchrony in power-grid networks. Nat Phys 2013;9(3):191–7.
[27] Carreras Benjamin A, Tchawou Tchuisseu Eder Batista, Reynolds-Barredo José M, Gomila Damià, Colet Pere. Effects of demand control on the complex dynamics of electric power system blackouts. Chaos 2020;30(11):113121.
[28] Carreras BA, Lynch VE, Dobson I, Newman DE. Complex dynamics of blackouts in power transmission systems. Chaos 2004;14(3):643–52.
[29] Mei Shengwei, He Fei, Zhang Xuemin, Wu Shengyu, Wang Gang. An improved OPA model and blackout risk assessment. IEEE Trans Power Syst 2009;24(2):814–23.
[30] Jovcic D, Ahmed K. High voltage direct current transmission: Converters, systems and DC grids. Wiley; 2019.
[31] Li Yang, Wu Shangsong. Controlled islanding for a hybrid AC/DC grid with VSC-HVDC using semi-supervised spectral clustering. IEEE Access 2019;7:10478–90.
[32] Jiang Han, Zhou Yichen, Gao Yi, Gao Shilin. Droop frequency limit control and its parameter optimization in VSC-HVDC interconnected power grids. Energies 2024;17(15).
[33] Fritzsch Julian, Colet Pere, Jacquod Philippe, Gomila Damià, Carreras Benjamin A. Stabilizing large-scale electric power grids with adaptive inertia. PRX Energy 2024;3:033003.
[34] Taher Halgurd, Olmi Simona, Schöll Eckehard. Enhancing power grid synchronization and stability through time-delayed feedback control. Phys Rev E 2019;100(6):062306.
[35] Ódor Géza, Hartmann Bálint. Heterogeneity effects in power grid network models. Phys Rev E 2018;98(2):022305.
[36] Ódor Géza, Deng Shengfeng, Hartmann Bálint, Kelling Jeffrey. Synchronization dynamics on power grids in Europe and the United States. Phys Rev E 2022;106(3):034311.
[37] Ódor Géza, Hartmann Bálint. Power-law distributions of dynamic cascade failures in power-grid models. Entropy 2020;22(6):666.
[38] Ahnert K, Mulansky M. Boost::odeint. 2012.
[39] Watts Herman, Shampine Lawrence, Burkardt John. R8_RKF45: Runge-Kutta-Fehlberg method for solving ordinary differential equations. 2004, https://www.gnu.org/software/gsl/. Modified version of the original FORTRAN77 by Herman Watts and Lawrence Shampine, adapted to C++ by John Burkardt.

[40] Schröder Malte, Timme Marc, Witthaut Dirk. A universal order parameter for synchrony in networks of limit cycle oscillators. Chaos 2017;27(7).
[41] Schäfer Benjamin, Witthaut Dirk, Timme Marc, Latora Vito. Dynamically induced cascading failures in power grids. Nat Commun 2018;9(1):1975.
[42] ENTSOE. HVDC links in system operations. 2019.
[43] Bianchi A, Nylander G. Operation and control of HVDC grids (dissertation). 2018.
[44] Beerten J. Modeling and control of DC grids Ph.D. dissertation, Faculty of Eng. Science, KU Leuven; 2013.
[45] Yan Kefei, Li Guoqing, Zhang Rufeng, Xu Yan, Jiang Tao, Li Xue. Frequency control and optimal operation of low-inertia power systems with HVDC and renewable energy: A review. IEEE Trans Power Syst 2024;39(2):4279–95.
[46] Bahrman MP. HVDC transmission overview. In: 2008 IEEE/PES transmission and distribution conference and exposition. 2008, p. 1–7.
[47] Hartmann Bálint, Ódor Géza, Benedek Kristóf, Papp István. Studying power-grid synchronization with incremental refinement of model heterogeneity. Chaos 2025;35(1).
[48] Xiong Bobby, Fioriti Davide, Neumann Fabian, Riepin Iegor, Brown Tom. Prebuilt electricity network for PyPSA-Eur based on OpenStreetMap data. 2024.
[49] Hörsch Jonas, Hofmann Fabian, Schlachtberger David, Brown Tom. PyPSA-Eur: An open optimisation model of the European transmission system. Energy Strategy Rev 2018;22:207–15.
[50] Benedek Kristóf. kuramoto2: Simulation code for quantitative and qualitative power-grid studies. 2025, https://github.com/NetworkingWithKuramoto/kuramoto2.